NMR study of a gel layer formed on an irradiated Na-aluminoborosilicate glass during aqueous alteration

Sathya Narayanasamy, Thibault Charpentier, Amreen Jan, Melanie Moskura, Matilde Benassi, Jean-Marc Delaye, Stephane Gin

npj | materials degradation

Article

Published in partnership with CSCP and USTB

https://doi.org/10.1038/s41529-024-00550-x

NMR study of a gel layer formed on an irradiated Na-aluminoborosilicate glass during aqueous alteration

Sathya Narayanasamy[1] ✉, Thibault Charpentier[2], Amreen Jan[1], Mélanie Moskura[2], Matilde Benassi[2], Jean-Marc Delaye[1] & Stéphane Gin[1]

Simplified borosilicate glass powders were irradiated by 952 MeV ^{136}Xe ions and then altered in a solution at a high S/V ratio at pH 9 and 90 °C for 33 days. Compared to the alteration of a non-irradiated sample, the irradiated sample altered 3–5 times more. Overall, both the gels had a similar structure as indicated by ^{29}Si, ^{27}Al, ^{23}Na, and ^{17}O NMR experiments. Nevertheless, according to ^{11}B and ^{1}H NMR experiments, differences were observed in the quantity and speciation of B retained in the gels. The results suggest that the glass alteration mechanisms responsible for passivation are not changed because of the irradiation-induced structural damages. However, the alteration kinetics, gel morphology related to porosity, and the degree of maturation are different. It seems that the gel formed on irradiated glass matures faster and retains B, which in turn influences the glass dissolution rate.

Radioactive waste, generated principally from the nuclear fuel cycle used for power generation, is classified based on the activity and the half-life of its radioactive constituents[1]. The radioactive waste, whose activity is in the order of several billion Bq/g, is classified as high-activity radioactive waste[2]. Many countries, including the USA, UK, France, Japan, China, and India, have decided to immobilize the high-activity radioactive waste by vitrification[1,3]. This results in the production of radioactive glass blocks, where the calcined radioactive fission products and actinides are mixed with borosilicate glass frit and melted together. The radioactive elements become a part of the borosilicate glass network, either as network formers or as modifiers, and thus immobilized[4,5]. Deep underground geological storage of these nuclear waste packages with multiple natural and engineered barriers is a viable long-term solution to their disposal[1,6]. Under such disposal conditions, eventually the radioactive glass will be exposed to water. Therefore, it is necessary to understand the behavior of glass under such circumstances. It is logistically challenging to conduct glass-water leaching experiments with radioactive glass samples and thoroughly characterize them. Therefore, studies are often conducted on simplified glasses and surrogate glasses that simulate the composition of radioactive glass but are inactive[7–12]. These studies help to understand the influence of different parameters such as glass composition, structure, water composition, pH, temperature, duration etc. on glass alteration kinetics and mechanisms. Glass typically reacts with water and forms an altered glass layer often characterized as a gel layer. Glass alteration and gel formation can be a result of a combination of mechanisms such as inter-diffusion, complete dissolution of silicate network, precipitation, partial network hydrolysis followed by in-situ condensation of silanol or hydrolyzed low-soluble species, gel-reorganization with time[13–16]. This gel layer might also play a crucial role in glass alteration kinetics. The composition and pore structure of the gel layer might influence the transport properties, affect the diffusion of water molecules and other species through the gel, and act as a passivation barrier that reduces the glass alteration rate over time[15,17–19].

An additional factor that can influence the glass alteration is the radiation damage in a radioactive glass sample, which contains alpha, beta, and gamma emitters that cause electronic excitation and ionization, and atomic displacements. The recoil nucleus from the alpha decay of the minor actinides in the glass causes significant structural modifications to the glass network. Detailed information about the radiation damage in nuclear waste glasses can be found in literature[5,20–23]. The radiation damages could be studied by either preparing actinide-doped simplified or surrogate waste glasses or by external irradiation of inactive glass samples. Both methods have their advantages and disadvantages. However, studying externally irradiated samples is less challenging.

A few studies compared the leaching of actinide-doped/irradiated glass samples with their inactive surrogates. The comparison showed that there are some notable differences in the alteration kinetics. The magnitude of the difference could vary depending on glass composition and other experimental parameters[22,24–29]. For example, the effect of alpha emitters on the initial glass alteration kinetics, studied using a comparison of actinide-doped R7T7 (the French reference nuclear waste glass) and its irradiated and inactive surrogates, was shown to be insignificant for the alteration (leaching) conditions (90 °C)[24]. Another study comparing ISG

[1]CEA, DES, ISEC, DPME, SEME, University of Montpellier, Marcoule, 30207 Montpellier, Bagnols-sur-Cèze, France. [2]Université Paris-Saclay, CEA, CNRS, NIMBE, 91191 Gif-sur-Yvette, Cedex, France. ✉e-mail: sathya.narayanasamy@cea.fr

(International Standard Glass), which was externally irradiated to simulate the damage induced by atomic displacements, with its non-irradiated pair showed that the initial glass dissolution rate increased by a factor of 2 (pH 9, 90 °C)[30]. The R7T7 glass and the ISG glass have very similar Si/B, Si/Na, Si/Al, Si/Zr, and Si/Ca molar ratios, but the R7T7 glass is a complex glass with approximately 30 oxides, and the ISG glass contains only six oxides. Another simplified glass having similar Si/B, Si/Na, and Si/Al molar ratios is the CJ2 glass, which is a quaternary borosilicate glass. The use of simplified glasses aids in a better comprehension of the influence of glass composition and other factors as well as in gaining insight into glass alteration mechanisms as there are fewer parameters that affect the overall result observed[9]. Since the objective of the study is to understand better the possible mechanistic differences in the glass alteration due to the structural differences induced by irradiation, CJ2 glass is well suited for this study.

Two earlier studies compared the CJ2 glass alteration between non-irradiated and irradiated glass[28,31]. One of these studies presented the comparison between the alteration of CJ2 glass irradiated by 7 MeV Au ions and its non-irradiated pair[31]. This study effectively showed that irradiation affects the inter-diffusion mechanism more than it affects the network-hydrolysis mechanism. The study also shows that the irradiation effect on hydrolysis diminishes with time because of a faster gel-reorganization of the irradiated glass[31]. The other study discussed the comparison between a CJ2 glass irradiated using 952 MeV ^{136}Xe ions prior to alteration and its non-irradiated pair[28]. Both the irradiation conditions mentioned above simulate the nuclear damages induced in the glass due to the ballistic effects of the recoil nuclei from the alpha decay of the minor actinides. However, the impact range for the 7 MeV Au ion is around ~2 µm, whereas it is ~63 µm for the 952 MeV ^{136}Xe ions. The latter study discussed in detail the structural damages inflicted by the irradiation and the effects it had on glass alteration. Briefly, the initial glass dissolution rate increased by approximately five times, and the normalized mass loss of boron over a longer alteration duration (33 days) increased by a factor of 1.7 to 2.5 times. The study concluded that even though the irradiation increased glass alteration rates, the alteration mechanism seems to be the same in both cases[28]. In addition, the authors also suggested that the gel-reorganization in the irradiated glasses could be faster. This study, which is complementary to the previous one[28], presents a similar experiment designed with the goal to understand and compare the gel structure, alteration mechanisms, and extent of reorganization. CJ2 glass powders of particle size between 6–8 µm were completely irradiated by 952 MeV ^{136}Xe ions (the same conditions as the previous study)[28]. The powders were then altered at high S/V 90 °C and pH 9 for 33 days in a solution enriched with ^{17}O. The gel layer formed during this alteration incorporated the ^{17}O from the solution, which was then probed by NMR analysis. The results were compared with the same experiment performed on the non-irradiated CJ2 glass powders. The study gives some insights into the potential differences caused by irradiation on the gel formation and maturation.

Results

Impact of heavy ions irradiation on glass structure

The previous study on the radiation effect on the alteration behavior of the CJ2 glass discusses in detail the impact of ~952 MeV ^{136}Xe heavy ions irradiation on the pristine glass structure[28]. Briefly, the irradiation made the glass more depolymerized. The ^{11}B MAS and MQMAS NMR data showed a strong decrease in the fraction of 4-coordinated BO_4^- species (B^{IV}) in the glass (48 ± 2% to 37 ± 2%). There is also a peak shift of the three-coordinated BO_3 species (B^{III}), which suggests that there is a higher B/Si mixing after irradiation. The ^{23}Na, ^{27}Al, and ^{29}Si MAS NMR spectra reflect the decrease in glass polymerization of the irradiated samples as well. The change in density was not measured accurately. Nonetheless, a decrease in density of the irradiated sample was observed qualitatively through a decrease in the refractive index determined by Spectroscopic Ellipsometry.

Impact of heavy ions irradiation on glass alteration

Figure 1 presents the SEM cross-sections of the irradiated and non-irradiated altered samples. The contrast in the presented images has been enhanced to improve the distinction between the unaltered glass core and the gel layer. All the acquired SEM images of the altered glass powders are presented in Supplementary Tables 1 and 2 in the supplementary data without any pretreatment. Due to the varying orientation of the grains, the gel layer thicknesses can only be estimated approximately from these SEM images. The altered layer thicknesses of the CJ2 Alt. (the altered CJ2 sample) varied from 170 nm to 660 nm approximately. The altered layer thickness of the CJ2 Irr. Alt. (the altered and irradiated CJ2 sample) varied between 870 nm to 2.22 µm. A few grains seemed to be altered to the core. However, this may be due to the orientation of the grain in the epoxy resin. These data translate to approximately 10–20 volume % alteration of the CJ2 Alt. sample and approximately 50–70 volume % alteration of the CJ2 Irr. Alt. sample. The alteration of the irradiated sample seems to be three to five times higher.

NMR analysis of altered glass powders

At the end of the alteration experiment, the recovered altered glass powders were rinsed in DI water through a vacuum pump filter. The recovered powders (approximately 70–80 mg) were packed in a rotor for NMR analysis and kept in the oven at 50 °C to evaporate intergranular water and the free water molecules in the pores of the gel layer. The mass loss with time was followed by periodically weighing the rotor. The mass loss curves are shown in Fig. 2 for the irradiated and non-irradiated samples. The rate of mass loss

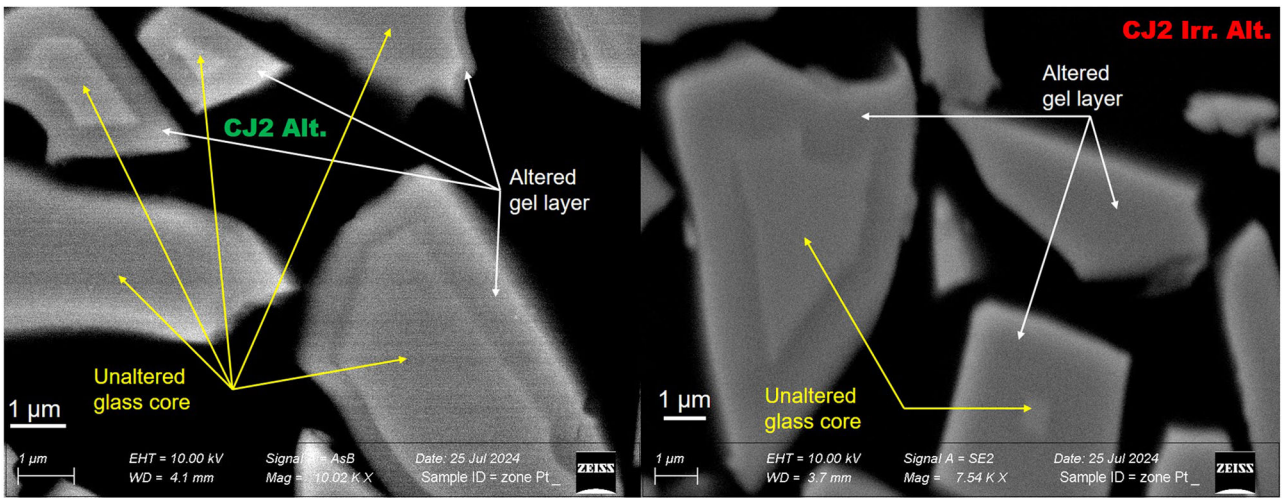

Fig. 1 | SEM cross-section images of altered glass powders. (Left) SEM image of the altered CJ2 glass powders. (Right) SEM image of the irradiated and altered CJ2 glass powders.

is the same for both samples up to a certain time (3 h). The mass loss is linear as a function of the square root of time until this point. After this, the rate of mass loss from the irradiated and altered sample slows down, deviating from linearity with respect to the square root of time. As the rate of mass loss in the irradiated sample seemed to reach saturation, the heating was stopped. The heating of the non-irradiated sample was continued for up to 7.5 h.

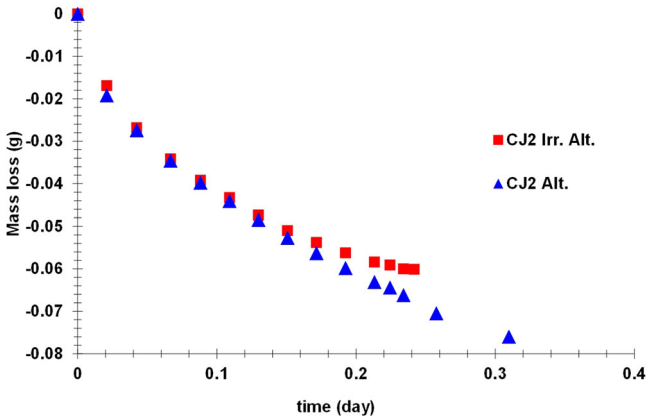

Fig. 2 | Mass loss from altered glass powders stored in the rotor in an oven at 50 °C.

Figure 3a shows the ^{11}B MAS NMR spectra of the irradiated and non-irradiated samples before and after alteration. Since the samples are not altered to their core, the signals in the altered samples come from boron in the unaltered fraction and hydrated boron that may be present in the gel layer or gel-glass interface. In the CJ2 Irr. Alt. sample, there is a contribution of the BO_4^- peak at positive NMR shifts (about 2 ppm) compared to the pristine glass ^{11}B MAS NMR spectra. This contribution is absent in the CJ2 Alt. spectra. This could mean that there is possibly a difference in the boron environment in the CJ2 Irr. Alt. sample and the CJ2 Alt. sample.

Interestingly, we note the presence of a narrow peak at 5 ppm that may correspond to tetra-coordinated borate complexes that have been observed in ionic liquids with a high concentration of boric acid[32]. This peak is only present in the CJ2 Irr. Alt. sample. Similarly, a peak at around 12.5 ppm is present only in the CJ2 Alt. sample but absent in the CJ2 Irr. Alt. sample. This could correspond to hydrated or aqueous tri-coordinated boron species such as $B_3O_3(OH)_4$[33]. For high mobility species (such as in a liquid) the width of the line is dominated by the quadrupolar T2 (transverse relaxation time, which is the time constant for the exponential decay of the transverse magnetization after an RF pulse). As BO_3 has a strong C_Q, versus BO_4, it could explain why the BO_3 peak is larger than BO_4. For both peaks, the

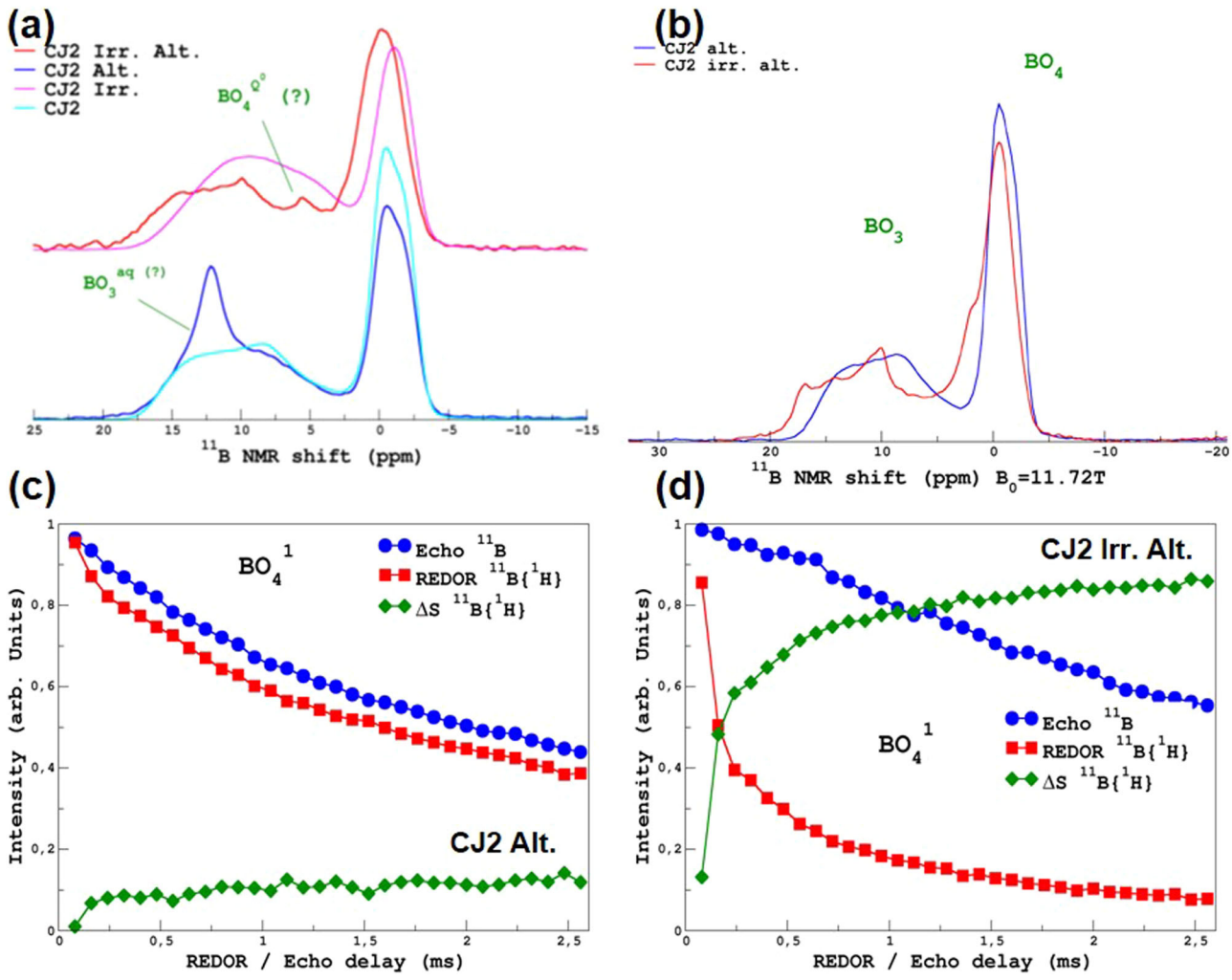

Fig. 3 | ^{11}B NMR spectra and REDOR data. a ^{11}B MAS NMR spectra of the unaltered irradiated sample (pink line), irradiated and altered sample (red line), the unaltered non-irradiated sample (cyan line), and the non-irradiated and altered sample (navy-blue line). **b** ^{11}B MAS NMR spectra of the irradiated and altered (red line) and the non-irradiated and altered sample (navy-blue line) after the samples were heated again at 50 °C. **c** ^{11}B Echo, ^{11}B {^{1}H} REDOR corresponding to the BO_4^1 component at ~ −0.5 ppm, and the delta for the non-irradiated and altered sample and **d** ^{11}B Echo, ^{11}B {^{1}H} REDOR corresponding to the BO_4^1 component at ~ −0.5 ppm, and the delta for the irradiated and altered sample.

question remains whether these two species form a part of the gel network or are present in the pore water. As is observed from ^{1}H and ^{17}O MAS NMR (vide infra) spectra shown later, a significant amount of liquid-like water (i.e., very narrow peak under MAS conditions) was present in the samples. The samples were placed again in an oven at 50 °C overnight in order to remove this "free" water.

Figure 3b shows the ^{11}B MAS NMR spectra acquired on the altered samples after the final heat treatment. These spectra show that in the CJ2 Alt. sample, the peak at 12.5 ppm is removed. This confirms that the altered gel layer had accessible pore water containing dissolved three-coordinated boron species before heating. The spectra now closely resemble the unaltered glass spectra. Similarly, in the CJ2 Irr. Alt. sample, the sharp peak at 5 ppm that was attributed to tetra-coordinated boron complexes is also removed. However, the peak seems to have shifted closer to 0 ppm assigned to BO_4 species. Despite the thermal treatment, there is still a significant difference between the unaltered (irradiated) glass spectra and the altered glass spectra. This confirms the retention of boron in the gel formed during the alteration of the irradiated sample. It also shows that the boron speciation/environment in the pore water of the gel is quite different between the two samples.

In order to further investigate the hydrated boron species, NMR REDOR experiments were performed as discussed in an earlier publication[34]. Briefly, the REDOR signals permit us to determine efficiently the fraction of one species associated with another. For close nuclei (few Å), a rapid increase of the REDOR signal is observed, whereas, for more distant nuclei (under our experimental conditions, can be estimated to be of the order of 10 Å), slow growth is observed (dephasing caused by distant proton atoms). Considering that these two cases correspond to species that are part of the altered glass, the plateauing value can be seen as a qualitative estimation of hydrated species. These two cases will be illustrated below. The ^{11}B MAS NMR spectra of unaltered glasses can be deconvoluted into four main contributions (BO_3^1, BO_3^2, BO_4^1 and BO_4^2). An additional BO_3-aq component was identified for the CJ2 Alt. sample. For the CJ2 Irr. Alt., in which the ^{11}B MAS NMR spectra show a shift in both the BO_3 component and the BO_4 component, BO_3-hyd, and BO_4-hyd components were identified additionally using cpMAS experiments (shown in Supplementary Fig. 1 in part 2 of the Supplementary Data). Figure 3c, d shows the ^{11}B {^{1}H} REDOR MAS NMR of the CJ2 Alt. and the CJ2 Irr. Alt. sample respectively for the BO_4^1 component (~−0.5 ppm). The REDOR curves associated with the other components are shown in Supplementary Fig. 2. These results show unambiguously that hydrated boron species are retained in the gel layer of the CJ2 Irr. Alt. glass. Although it is difficult to ascertain an exact fraction, it seems that a majority of the ^{11}B signal from the irradiated and altered sample is from the hydrated gel layer. To explore this point further, deconvolution of the ^{11}B MAS NMR spectra of the samples before the second heating was performed (supplementary Figs. 3 and 4) by regrouping the BO_3^1 and BO_3^2 components into a single BO_3 component for the glass and likewise for the merged BO_4 component. In the case of the non-irradiated and altered sample, 20% of spectra were from the BO_3 (aq) peak at ~12.5 ppm, which disappeared after the second heating. In the case of the irradiated and altered sample, 36% of the signal corresponds to hydrated BO_4 species, and 24% of the signal corresponds to hydrated BO_3 species. Therefore, 60% of the boron signal seems to be from the gel layer. Considering that the boron concentration in the gel and the glass is probably different and the boron retention in the gel layer is not known, this cannot be directly attributed to an altered glass fraction.

Figure 4a shows the ^{23}Na MAS NMR spectra of the irradiated and non-irradiated CJ2 samples before and after alteration. The NMR spectra of ^{23}Na in a hydrated environment, i.e., in the altered layer, typically show a peak that is narrower than the spectra in unaltered glass and displays a higher MAS chemical shift[34,35]. This is the case in this study as well. Because of the reduction of the line-width upon hydration, the spectra easily allow distinguishing between Na signals from pristine glass and the Na signals from the gel. This is more evident in the CJ2 Alt. sample, where the altered glass percentage is low (thus with a strong pristine glass component). Supplementary Fig. 5 in the supplementary data shows the deconvolution of these spectra, which indicates that the altered glass fraction of the CJ2 Alt. the sample is 24%, and that of the CJ2 Irr. Alt. sample is 79%. The Na concentration in the gel layer is lower than its concentration in the pristine glass. Therefore, this cannot be attributed directly to an altered glass fraction. However, considering that both samples might have the same Na percent in the gel layer, the CJ2 Irr. Alt. has a higher fraction of altered glass. The spectra also show a sharp peak at 0 ppm, characteristic of Na in an aqueous environment (0.1 M NaCl aqueous solution is used as a reference for ^{23}Na chemical shift at 0 ppm). This peak disappears when the samples are heated, as shown in Fig. 4b. The ^{23}Na MAS NMR peak of the heated CJ2 Irr. Alt. sample shows some additional small peaks at 1 ppm and −5 ppm, which remain unexplained. It might be possible that the Na speciation slightly changed during the heating of the altered samples, or it could be due to the formation of some sodium carbonate-type secondary phases with the formation of NaO_6 and NaO_7 type configurations[36,37].

Figure 4c shows the ^{27}Al MAS NMR spectra of the irradiated and non-irradiated samples before and after alteration. Similar to Na, the ^{27}Al MAS NMR spectra are typical of altered glasses[17,34,38]. The peak of Al in a more hydrated environment is narrower than in glass, with a slightly higher MAS chemical shift. The presence of water molecules, which are subjected to vibrations, close to aluminum, decreases the effective electric field gradient and, consequently, the quadrupolar interaction and line-width of the ^{27}Al MAS NMR spectra. The difference in intensity of the two components (broad: pristine glass; narrow: altered glass) between the unaltered and altered spectra also corroborates well with the fraction of altered glass in the irradiated and non-irradiated samples. An attempt was made to decompose the ^{27}Al MAS NMR spectra to identify the contribution from the gel layer and the remaining unaltered glass (Supplementary Fig. 6). It seems that the fraction of the altered glass is overestimated, as the results indicate that the altered glass fraction of the CJ2 Alt. sample is 50% and that of the CJ2 Irr. Alt. is 100%. This is higher than what is estimated through the deconvolution of the ^{23}Na MAS NMR spectra (Supplementary Fig. 5). The reason for this difference is not clear. No differences were observed in the spectra after heating (spectra not shown here), suggesting that there is no Al accessible to the pore water of the gel layer. Figure 4d, e shows the ^{27}Al {^{1}H} REDOR MAS NMR of the CJ2 Alt. and the CJ2 Irr. Alt. sample respectively. These results, in line with the ^{11}B {^{1}H} REDOR, show that less than 10% of the ^{27}Al in the CJ2 Alt. sample is in close proximity to ^{1}H and that ~50–60% of the ^{27}Al in the CJ2 Irr. Alt. the sample is in close proximity to ^{1}H. This again confirms that the CJ2 Irr. Alt. the sample has a higher fraction of altered glass.

As suggested above, the ^{1}H MAS NMR spectra shown in Fig. 5a corroborate the presence of pore water in the CJ2 Alt. sample. Figure 5b shows the ^{1}H MAS NMR spectra acquired at two different spinning frequencies and under static (i.e., non-spinning) conditions. The presence of strong spinning sidebands and the increase in the ^{1}H peak width at a very low spinning rate support the confinement of the water at a meso/nano-scale[39,40]. In the CJ2 Irr. Alt. sample, there does not seem to be a significant amount of pore water, but there is an indication of the presence of free water within the gel and silanol and Al-OH species. Figure 5c shows the ^{1}H MAS NMR spectra of the altered samples after heating to remove the excess pore water. As expected, the sharp peak corresponding to the pore water has disappeared. However, the spectra are quite different between the gel formed on a non-irradiated glass and irradiated glass. The mean resonance that can be assigned to molecular water is shifted. Figure 5d, e shows the ^{1}H MAS NMR–Hahn-Echo (HE) spectra with increasing echo delay values of the CJ2 Alt. and CJ2 Irr. Alt. samples respectively. The Hahn-Echo-pulse sequence comprises initially a 90° pulse to excite the nuclear spins followed by a 180° pulse after a time delay (τ) to refocus the dephased spins. The echo is formed at time 2τ. When the 90° RF pulse is applied, the ^{1}H nuclear spins are aligned perpendicular to the static magnetic field resulting in a transverse magnetization and the detectable NMR signal. Afterwards, the nuclear spins begin to go out of phase with each other due to spin-spin interaction and the local electronic environment, resulting in a decreased signal intensity. If the H concentration is higher with more H-H interaction (dipolar magnetic

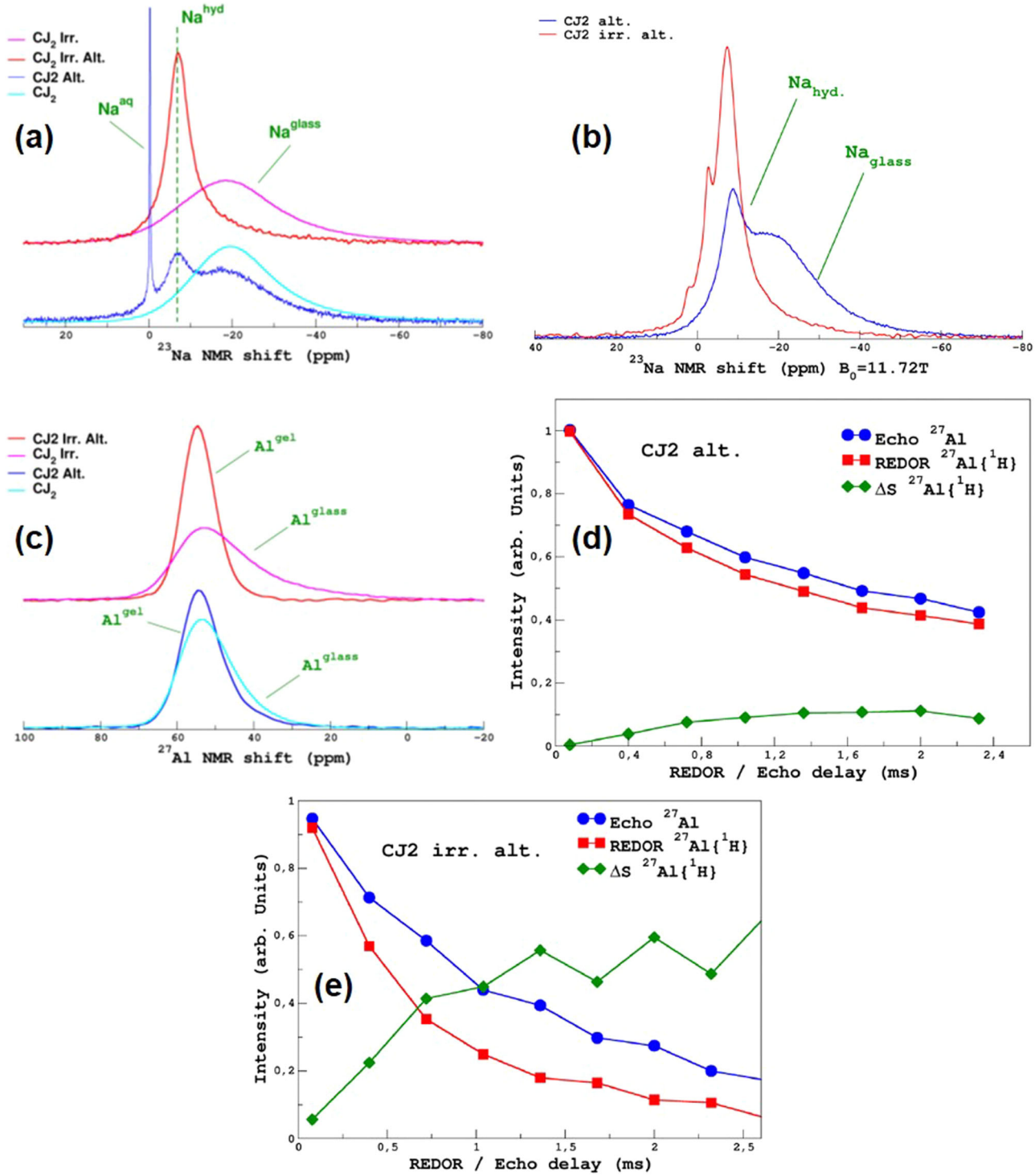

Fig. 4 | ^{23}Na and ^{27}Al MAS NMR and REDOR data. a ^{23}Na MAS NMR spectra of the unaltered irradiated sample (pink curve), irradiated and altered sample (red curve), the unaltered non-irradiated sample (cyan curve) and the non-irradiated and altered sample (navy-blue curve). **b** ^{23}Na MAS NMR spectra of the irradiated and altered (red line) and the non-irradiated and altered sample (navy-blue line) after the samples were heated again at 50 °C. **c** ^{27}Al MAS NMR spectra of the unaltered irradiated sample (pink curve), irradiated and altered sample (red curve), the unaltered non-irradiated sample (cyan curve), and the non-irradiated and altered sample (navy-blue curve). **d** ^{27}Al Echo, ^{27}Al {^{1}H} REDOR, and the delta for the non-irradiated and altered sample, and **e** ^{27}Al Echo, ^{27}Al {^{1}H} REDOR, and the delta for the irradiated and altered sample.

interactions), the decrease in the signal intensity occurs faster (faster T2-spin-spin relaxation time). Thus, the echo signal after the time delay gives information about the interactions between the protons in the sample. For a short τ, the echo signal is relatively strong and might resemble the ^{1}H MAS NMR spectra. For a longer τ, the dipolar interactions between the protons dephase the proton spins and result in a decreased signal intensity. Therefore, for the same echo delay, higher H-H interactions (that can be related to proton density) will result in a higher decrease in the signal intensity. In the CJ2 Alt. sample, the variation of the echo delay results in a strong decrease of the molecular water peak, allowing the resolution of the hydrogen-bonded

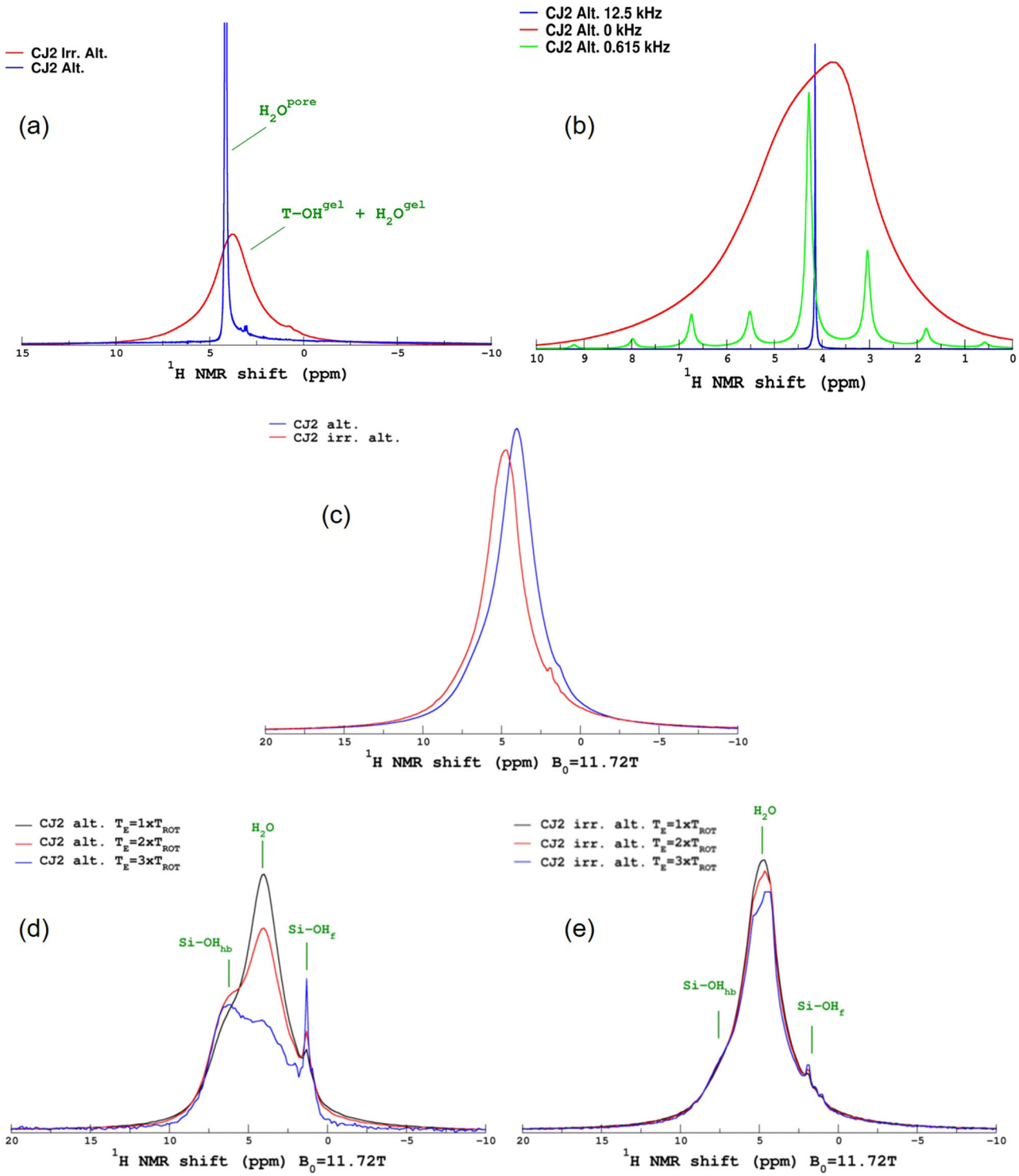

Fig. 5 | ^{1}H MAS NMR spectra. a ^{1}H MAS NMR spectra of the irradiated and non-irradiated altered samples. **b** ^{1}H MAS NMR spectra of the non-irradiated and altered sample at different spinning frequencies. **c** ^{1}H MAS NMR spectra of the irradiated and non-irradiated altered samples after heating again at 50 °C. **d** ^{1}H MAS NMR–Hahn-Echo spectra with varying echo delay of the non-irradiated and altered sample. **e** ^{1}H MAS NMR–Hahn-Echo spectra with varying echo delay of the irradiated and altered sample.

(hb) silanol species and isolated silanol (f) peaks. In contrast, in the CJ2 Irr. Alt. sample, there is no change in the line shape, suggesting a weaker proton network in terms of H-H distances and, thus, weaker hydrogen bonds.

Figure 6a, b presents the ^{17}O MAS NMR spectra of the non-irradiated and irradiated altered samples. As a reminder, the unaltered glass samples were not enriched in ^{17}O, but they were altered in a solution enriched in ^{17}O (90%). Therefore, the ^{17}O observed in the altered samples results exclusively from the incorporation and reactivity of the alteration solution within the gel network. The CJ2 Alt. sample presents a very sharp and intense peak confirming the presence of nanoporous water in this sample. Figure 6c presents the ^{17}O MAS NMR spectra acquired after additionally heating the sample at 50 °C to remove the pore water. The spectra of the CJ2 Alt. and CJ2 Irr. Alt. are remarkably very close in shape, and differ in the relative fraction of Si-OH. Figure 6d shows the Hahn-Echo observations. The echo

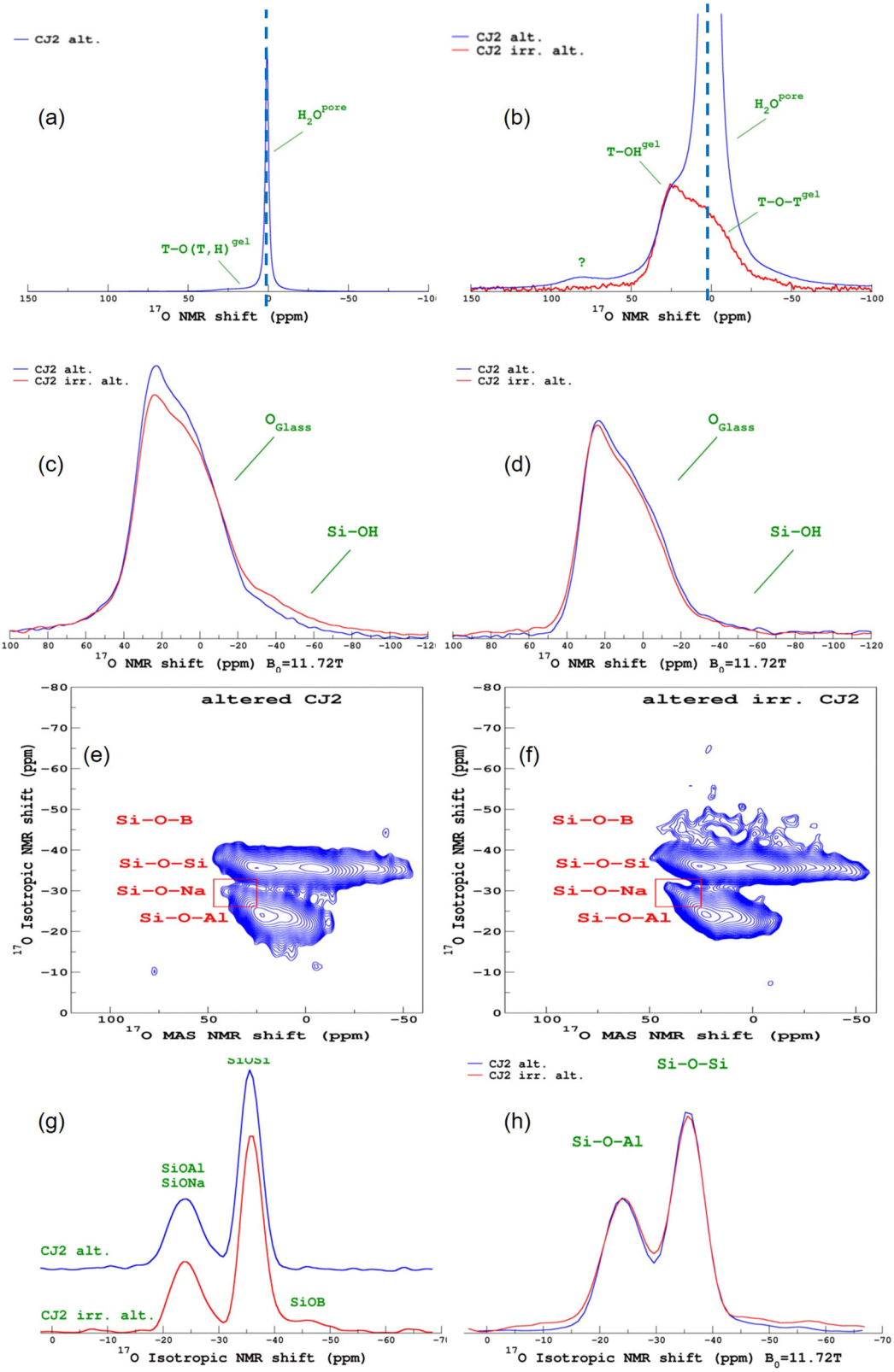

Fig. 6 | ^{17}O MAS and MQMAS NMR spectra. a ^{17}O MAS NMR spectra of the non-irradiated and altered sample. **b** ^{17}O MAS NMR spectra of the non-irradiated and irradiated altered samples. **c** ^{17}O MAS NMR spectra of the non-irradiated and irradiated altered samples after heating again at 50 °C. **d** ^{17}O MAS NMR–Hahn-Echo observation spectra of the non-irradiated and irradiated altered samples after heating at 50 °C. **e** ^{17}O MQMAS NMR spectra of the non-irradiated and altered sample before heating. **f** ^{17}O MQMAS NMR spectra of the irradiated and altered sample before heating. **g** Isotropic projection of the ^{17}O MQMAS NMR spectra of the non-irradiated and irradiated altered samples before heating. **h** Isotropic projection of the ^{17}O MQMAS NMR spectra of the non-irradiated and irradiated altered samples after heating.

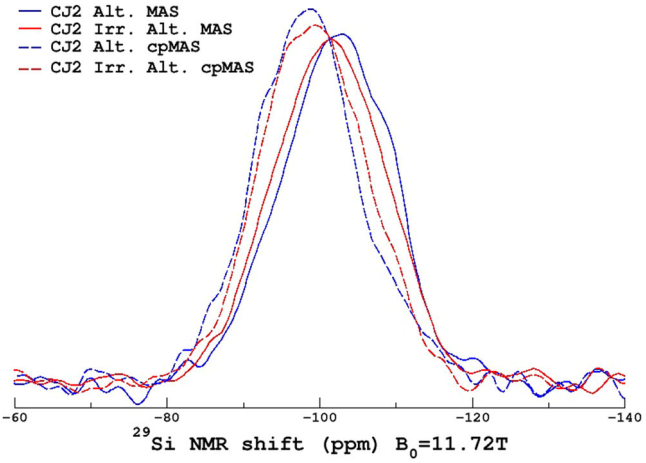

Fig. 7 | ^{29}Si MAS NMR spectra of the non-irradiated and altered and irradiated and altered glass powders.

causes the Si-OH component to be strongly attenuated. The decrease is ascribed to the strong dipolar coupling between ^{17}O and ^{1}H in the Si-OH pair[41,42].

Apart from this, both the irradiated and the non-irradiated samples show evidence of the formation of (Si, Al)-^{17}O-H, (Si, Al)-^{17}O-(Si, Al), suggesting the recondensation of the less soluble glass network formers within the gel layer. Figure 6e, f show the ^{17}O MQMAS NMR spectra of the altered samples. Note that in such experiments, the (Si, Al)-OH components are filtered out. In both the non-irradiated and irradiated samples, the presence of Si-^{17}O-(Si, Al, and Na) can be seen. Only in the CJ2 Irr. Alt. sample, a weak signal of Si-^{17}O-B is observed, indicating that a small proportion of boron recondensed within the gel layer. The presence of Si-^{17}O-B in the CJ2 Irr. Alt. the sample is better observed in the isotropic projection of the MQMAS spectra shown in Fig. 6g. The isotropic projection of the MQMAS spectra obtained after the samples were heated at 50 °C are presented in Fig. 6h. There seem to be differences between the ratio of the Si-O-Si and Si-O-Al peaks and the signal for the CJ2 Irr. Alt. the sample seems more attenuated in the Si-^{17}O-B region. However, this difference is mainly due to the acquisition conditions of the spectra. The spectra in Fig. 6g were acquired with a MQMAS shifted echo (2 ms) pulse sequence[43], and the spectra in Fig. 6h were acquired with a Z-filter sequence[44]. This highlights the precautions needed while attempting to quantify the Si-O-X (X=Si, Al, B) fractions. Supplementary Fig. 7 shows a comparison of different acquisition conditions on the CJ2 Irr. Alt. sample after the second heating. Nonetheless, there are no remarkable differences in the ^{17}O environment of the CJ2 Irr. Alt. before and after heating.

Moreover, the oxygen environment is very similar in the two samples (CJ2 Alt. and CJ2 Irr. Alt.) as shown in Fig. 6h. These results show that the gel networks of the sample that was irradiated and altered and non-irradiated and altered are nearly identical in terms of Si/Al mixing, thus recondensation mechanisms are the same in both samples.

Figure 7 shows the ^{29}Si MAS and cpMAS spectra of the altered samples. The spectra indicate that the overall gel structure is similar and any minor differences might be attributed to differences in the altered glass percentage.

Discussion

Impact of heavy ions irradiation on glass structure

In this study, the radiation dose (~73 MGy) is above the "saturation dose" (estimated to be ~26 MGy) at which the structural changes induced by irradiation attain a maxima[20,21,23]. The high energy of the irradiating ^{136}Xe ions and the long impact range simulate the nuclear damages induced in the glass due to the ballistic effects of the recoil nuclei from the alpha decay of the actinides. Another study focusing on the effect of irradiation on glass alteration of the same glass used a lower energy ion with a much lower range (7 MeV Au ions, fluence of 2×10^{14} at/cm^3, impact on first two microns of the material, radiation dose ~40 MGy)[31]. This study also simulates the nuclear damages in a radioactive glass. It seems that the damage due to irradiation in both studies is consistent, although the intensity of the Raman peaks in the study with the lower dose of irradiation indicate that the damages might be to a lesser extent[31]. The higher energy of the irradiating ions in this study might have left tracks along its trajectory in the glass. This potentially augments the structural damage due to irradiation. In an actual radioactive glass, the incorporated minor actinides do not leave such irradiation tracks[20,22,23]. The range and energy of the recoil nucleus are much smaller than that of the ^{136}Xe ions used in this study.

Impact of heavy ions irradiation on glass alteration

In this study, the irradiated glass is altered approximately three to five times more than the non-irradiated glass. In the previous study conducted on the same glass with the same irradiation conditions[28], a similar 33-day long experiment was conducted on monoliths. The main differences are the S/V ratio (1 vs. 142 cm^{-1}) and solution composition. In the previous study, the solution was close to saturation with respect to amorphous silica—and likely at saturation with respect to the aluminosilicate gel that forms on the glass—since the beginning of the experiment, whereas in this study, the initial solution did not contain Si. In the previous study[28], the alteration increased by a factor of 1.7 to 2.5, which is lower than the three to fivefold increase in this study. However, the initial glass dissolution rate measurement carried out in dilute solutions showed an increase in alteration by a factor of 5.6 for the previous study. Therefore, the impact of irradiation on alteration in this study is closer to the impact on the initial glass dissolution rate than the glass alteration rate under saturated conditions. The higher S/V ratio in this study would have resulted in a rapid saturation of the solution with respect to aluminosilicate gel. However, the alteration in the initial few hours, before Si concentration reached saturation, was probably sufficient to ensure an overall higher observed effect of irradiation.

The effect of irradiation on glass alteration is dependent on glass composition and irradiation conditions[22,26,27,31,45,46]. Therefore, the comparison is not straightforward. Nevertheless, studies show that the internal or stored energy of the irradiated glass is higher[20,47,48]. The alteration kinetics of the irradiated or damaged glass is also higher. For the simpler glass compositions such as CJ2 and ISG, the effect of irradiation on glass alteration kinetics seems to be higher, especially the short-term alteration rates[30,31]. When studying the effect of irradiation and doping with ^{244}Cm on glass structure and the long-term alteration rate, it was shown that the ISG glass with the same Si/Al, Si/Na, Si/B molar ratios as the SON68 glass, was a good surrogate[22]. However, at short experimental durations, the effect of irradiation on glass alteration kinetics was more pronounced in the ISG than in the SON68[30]. Experiments designed specifically to observe the effect of irradiation on glass alteration mechanisms have shown that there is a more pronounced effect of irradiation on the inter-diffusion mechanism than the network-hydrolysis mechanism[31]. This is attributed to the fact that irradiated glass has more free volume due to swelling. It is around 1.91 ± 0.25% for the CJ2 glass (data not yet published, but measurement acquired using the same method in the cited literature[21,30,49]) and around 1.7% for the ISG glass[30], both irradiated under the same condition as the cited literature (7 MeV Au ions)[31]. For the irradiation conditions in this study, the increase in free volume was not measured accurately, but the decrease in density was observed[28]. The increased free volume might allow more water diffusion into the glass[50]. The inter-diffusion mechanism for the CJ2 glass consists of boron dissolution, which facilitates Na leaching[31]. Similar mechanisms may be controlling the residual glass alteration rate[9].

Under the alteration conditions in this study (pH 9, high S/V ratio, 90 °C, initially dilute conditions), both network-hydrolysis as well as inter-diffusion mechanisms would have occurred. Therefore, it is not possible to unravel the irradiation effect on a particular mechanism.

Impact of heavy ions irradiation on gel structure

The results presented in this study give some strong indications that the structure of the gel layer formed on the irradiated glass is close to that of the

gel layer formed on a non-irradiated glass. This is shown by the ^{17}O, ^{23}Na, ^{27}Al and ^{29}Si NMR experiments, which show similar environments for hydrated sodium and aluminum, a similar aluminosilicate network structure in both gels despite the significant variation in the glass alteration rate.

However, some results (notably ^{11}B MAS NMR spectra) show that the gel layer formed on the irradiated glass is quite different from the gel layer formed on a non-irradiated glass in certain aspects. The noticeable differences are discussed below.

The primary difference lies in the retention and speciation of boron in the gel layer. As evidenced by the presence of narrow peaks associated with free water (^{1}H MAS NMR) dissolved (i.e., liquid-like) Na (^{23}Na MAS NMR) and three-coordinated boron species (^{11}B MAS NMR), the gel layer of the non-irradiated altered sample contained a notable amount of pore water. After the second overnight heating of the samples (to remove all the pore water), the ^{11}B MAS NMR spectra closely resembled that of the unaltered sample. This suggests that almost all the boron from the gel layer is lost. The ^{11}B-^{1}H REDOR experiments, too, showed that there was not a significant amount of ^{11}B in the close proximity of ^{1}H in the sample.

On the other hand, the gel layer of the irradiated altered sample, although devoid of pore water at initial conditions of NMR measurements (as confirmed by ^{1}H MAS NMR spectra), still contains a small amount of hydrated four-coordinated boron species (^{11}B MAS NMR). ^{17}O MQMAS spectra showed signals of Si-^{17}O-B species, indicating that the boron in the gel layer hydrolyzed and recondensed within the gel layer with ^{17}O from the leaching solution. The ^{11}B MAS NMR spectra acquired also indicated the presence of boron species that were clearly distinct from those present in the irradiated and unaltered glass and were four coordinated. The additional heating modified the environment of the hydrated four-coordinated boron species observed earlier in the gel layer. This shows that a significant amount of boron is retained in the gel layer formed on the irradiated and altered glass. These results highlight two phenomena that are less common and less known (and therefore less discussed in the literature) that would merit a deeper discussion: boron retention in the gel layer and apparently different boron speciation in the gel layer due to irradiation.

Boron retention in the gel layer is relatively unusual during the alteration of a borosilicate glass. Boron is an element with very high solubility limits in aqueous solution. It is, therefore, generally used as a tracer of glass alteration along with Na when it is not involved as a charge compensator for other species such as Al^{IV} or Zr^{VI}. However, recent ToF-SIMS analyses of altered monoliths have shown that boron can be retained in the gel layer. This has been observed especially during the alteration of irradiated glasses[27,28,31], glasses altered for a long duration[51,52], and certain glass compositions[19,53]. It seems that, in all these cases, the alteration solution concentration was far from saturation with respect to boron-related secondary phases. Therefore, the retention of boron in the gel layer is probably related to an inability of the boron to migrate out of the gel layer. It can be hypothesized that boron retention in the gel layer is linked to gel maturation unless it is an effect of glass composition. The gel layer formed during glass alteration can be characterized as "dynamic", if gel restructuring advances rapidly or it can be characterized as "mature", if the gel restructuration is lower. This phenomenon was studied and demonstrated by altering ISG gels of different ages in isotopically marked water[54]. The gel maturation process can also refer to the evolution of the porous nature of the gel layer. In general, a gel layer initially formed has smaller pores, and with progressing alteration, the pore-size increases and the overall porosity decreases[55,56]. The evolution of porosity is also probably correlated to the restructuration dynamics of the gel layer.

The boron that is dissolved at the gel-glass interface must diffuse through the gel layer either through the pore channels and open porosity or through the gel layer itself, whose restructuration may create pathways for boron to diffuse out of the gel layer. In literature, it has been shown that while a nanoporous graphene membrane with a pore size of around 0.36 nm can effectively filter out three-coordinated hydrated $B(OH)_3$, a pore size of around 0.84 nm can allow at least some of the hydrated $B(OH)_3$ to pass through[57]. Therefore, it would seem that the pore channels in the gel layer should be at least around 1 nm to allow the diffusion of hydrated $B(OH)_3$. It can be postulated that while a young gel might be dynamic enough for the diffusion of hydrated boron species through the gel layer towards the leaching solution, an older gel or mature gel might not continue to reorganize itself to allow the passage of boron through breaking and reforming its Si-O-Si/Si-O-Al bonds. The boron diffusion through the gel layer towards the solution in a mature gel might be limited to the available open pore channels greater than 1 nm in diameter, resulting in at least a partial retention of boron in the gel layer.

While gel maturation generally progresses with time[55], it can be faster or slower depending on the initial pore volume created by the depart of the soluble elements (hence inducing a composition effect)[19,53]. Accordingly, the irradiated altered glass might have a higher initial pore volume due to swelling, and therefore, might mature faster. If the rate of gel maturation is dependent on the rate of glass alteration, then it may also be a possible explanation for boron retention in the gel layer formed on the irradiated glass. Experiments on the alteration of irradiated and non-irradiated ISG glass samples at 90 °C and pH 9 have shown that the gel layer formed on an irradiated glass does effectively mature faster[58]. The study also shows that the gel layers formed on the non-irradiated glasses also reach a similar state of maturation but after a longer alteration duration.

Regarding the boron speciation, it seems that the gel layer formed on the irradiated glass contains hydrated four-coordinated boron species in the pore water, whereas, in the non-irradiated glass, only three-coordinated boron seemed to be present. This is despite the fact that before glass alteration, the irradiated glass contained less four-coordinated boron. Such four-coordinated boron species in the gel layer have not been observed before. Even in a case where NMR analysis was performed on a boron-retaining gel formed on a non-irradiated glass during alteration in an unsaturated vapor phase[34], the boron speciation was different. These results highlight the necessity to study boron speciation in the gel layer over the course of drying.

Boron speciation in solution is dependent on pH, boron concentration, and even the presence of Na and Ca, which may form complexes with hydrated boric acid species[32,33]. It is complicated to examine pH effects in nanoconfined pore water. However, if the gel maturation entraps the hydrolyzed boron within the gel layer, then it is conceivable that the boron speciation might vary due to a higher boron retention within the gel layer or pore water. The higher fraction of SiOH in the gel layer of the irradiated glass may also play a role in determining the boron speciation. If the pH in pore water was increased due to a higher fraction of –OH endings in the gel layer, then that may also be responsible for the different boron speciation. It is unclear if the different boron speciation is an effect of the pre-irradiation or not. For clarity, NMR analysis would have to be performed on a boron-retaining gel that was formed under similar conditions on a non-irradiated glass.

The next difference is noticeable in the ^{1}H MAS NMR-Hahn-Echo spectra with varying echo delay. The ^{1}H MAS NMR of the non-irradiated and altered glass displays a standard behavior observed in the literature on the gels of non-irradiated and altered glasses[17,54]. With an increasing delay, the area under the spectra decreases (especially at the molecular water peak position at around 5 ppm), giving the possibility to estimate the water content percentage in the gel[54]. The irradiated and altered sample does not show the same decreasing behavior with the echo time. In brief, it suggests that the hydrogen bonds are weaker in the gel layer of the irradiated and altered sample. Literature on the adsorption studies on porous materials suggests that there may be differences in the interaction between a porous adsorbent and adsorbate depending on the pore structure. When the pore size is smaller, there is a stronger interaction between the pore walls and the diffusing/adsorbing species[59,60]. Therefore, this noticeable difference in the ^{1}H MAS NMR–Hahn-Echo spectra suggests a different pore morphology of the gel layer formed on the irradiated sample, likely with a larger average pore size. In the initial glasses before alteration, the density decreases with irradiation because of swelling[28]. It has been shown in the literature that during the alteration of the CJ2 glass, the gel layer forms by a mechanism of in-situ aluminosilicate network-hydrolysis and condensation, accompanied

by loss of boron and network modifying sodium ions through hydrolysis/inter-diffusion mechanism[16]. Consequently, the first gel formed by this mechanism "inherits" structural features from the glass. This could result in a gel layer formed on the irradiated glass that might have a higher porous volume because of the swelling (i.e. density decrease). The previous study that presents some TEM images of the CJ2 monoliths altered for 33 days suggested that the irradiated and altered sample seems to have better-defined pores than the non-irradiated and altered sample[28]. Another study on the ISG glass irradiated with 7 MeV Au ions also showed that the irradiated and altered sample was more porous for the same duration of alteration as its non-irradiated pair[58].

A more porous gel with larger pores might also explain the higher alteration kinetics of the irradiated and altered sample. It has been shown in the literature that a gel formed during alteration at pH 7, which contained a higher fraction of larger pores, altered faster than a gel formed at pH 9 with a smaller average pore size[56]. In the cited study[56], it was shown that the two gels also showed differences in the hydrous species present within the gel layer and that the gel with the larger pores had weaker hydrogen-bonded species.

Another study also discussed the differences in the hydrous species in the gel layer depending on the pH of the alteration solution[52]. The slight positive shift in the peak of the ^{1}H MAS NMR of the irradiated and altered samples could be because of a higher fraction of the hydrogen bonded Si-OH and some differences in the nature of the hydrous species.

In summary, according to the previous study[28], irradiation of the CJ2 glass resulted in (i) a decrease in the glass network polymerization, (ii) increase in the fraction of three-coordinated boron in the glass, and (iii) decrease in density. These changes resulted in an increased glass alteration during the 33 days of alteration. The overall gel structure seems to be similar to a gel formed on a non-irradiated glass, suggesting that the mechanism of formation of both gels must be similar. However, the gel seems to show differences in pore morphology with a potentially higher pore size for the irradiated and altered sample. Moreover, unlike the gel formed on non-irradiated glass, the gel retains boron, which can be considered as a sign that the gel is more mature. In other words, the gel is more reorganized and might be more passivating, i.e., it reduces the alteration rate considerably. The speciation of the retained boron was also different.

In concurrence with several studies[27,28,31,50], it is certain that the gel layer of an irradiated glass will attain maturation/passivation faster. At longer alteration durations, this passivation might lead toward minimizing the overall difference in the alteration kinetics between irradiated glass and non-irradiated glass. The exact mechanism that triggers this earlier passivation is unclear. It could be the initially higher void volume due to swelling, which promotes a faster reorganization. It could also be a consequence of the faster alteration. The role played by the retained boron on passivation remains to be clarified as well. It is likely an effect of gel maturation, which entraps at least some boron within the gel layer. However, the question remains if there exists a feedback mechanism of boron retention in the gel layer on alteration kinetics.

It should also be considered that these studies were conducted in a static environment. The passivation effect of the gel layer is dependent on the alteration environment. It has been shown in the literature that a gel layer that is already considered passivating might become unstable under certain conditions. For example, if the alteration environment becomes conducive to the formation of secondary phases such as silicates, then this triggers the dissolution of the gel layer to form precipitates[61,62]. Therefore, a thorough understanding of the alteration environment is crucial for the prediction of the long-term behavior of radioactive glass.

In this study, the gel structure formed on an irradiated glass was studied using NMR characterization to gain insights into the effect of the structural damage inflicted by the alpha emitters. There are several aspects to be explored before a complete understanding of the gel structure of a radioactive glass can be obtained. The effect of structural changes by other types of irradiation, a coupled effect between the pre-existing structural damage due to irradiation, and ongoing modifications in the gel structure due to radioactive elements entrapped in the gel layer remain to be further explored and understood.

Experimental methods

The Na-aluminoborosilicate glass used in this study is called CJ2, and its composition in mole percent of oxides is as follows: 64.9 SiO_2–17.3 B_2O_3–13.6 Na_2O–4.1 Al_2O_3. The glass synthesis is described in the literature[28]. Briefly, the glasses were synthesized using the melt-quench method at 1450–1500 °C, followed by an annealing step. The synthesized glass block is homogeneous. The granulometry of the glass powder used for alteration with or without irradiation is between 6–8 µm. The geometric surface area of the powders is 3564 $cm^2 g^{-1}$.

Irradiation of pristine glasses

The irradiation carried out at the beamline SME at GANIL facility in Caen is described elsewhere in more detail[28]. Briefly, ~952 MeV (7 MeV u^{-1}) ^{136}Xe ions were used for irradiation at a fluence of 7.5×10^{12} ion cm^{-2}. Normal incidence heavy ions (^{136}Xe) at room temperature irradiated the cleaned glass powders pasted using carbon tape onto aluminum sample holders. The range of irradiation is ~64 µm. Therefore, the heavy ions irradiated the grains homogeneously. The radiation dose received by the powder sample is equal to approximately ~73 MGy.

Alteration of non-irradiated and irradiated glasses

Hereafter, CJ2 refers to the non-irradiated CJ2 glass powders and CJ2 Irr. refers to the irradiated CJ2 glass powders. The alteration solution consists of an isotopically enriched water (90.7% ^{17}O) adjusted to pH 9 at 90 °C. The pH was adjusted using LiOH (0.00045 mol/L). The alteration duration is 33 days. The reactor is a perfluoroalkoxy (PFA) container with precautions in place to avoid solution loss due to evaporation. The S_{GEO}/V (geometric surface area of the glass powder divided by the solution volume) ratio of the experiment is 142.6 cm^{-1}. The geometric surface area of the glass powders was calculated by considering that the glass powders are spherical[63]. Considering that the actual surface area of the glass powders, if measured with BET, might be approximately two times higher, the true S_{BET}/V ratio is also approximately two times higher[64]. Considering the results available in the literature for the alteration of the CJ2 glass at 90 °C and initially pure water at a much lower S_{BET}/V ratio (80 cm^{-1}), the glass alteration rate dropped by a factor of 30 compared to the initial rate after 28 days of alteration[9]. Due to the higher S/V ratio in the current study, the alteration solution will attain saturation rapidly with respect to amorphous silica, with very little fraction of altered glass. The glass alteration rate is also expected to rapidly decrease and attain a steady state that is approaching the residual glass alteration rate[8]. Although the alteration kinetics will not be followed over time, the gel layer at the end of the experiment can be compared to a gel layer that is young, but with passivating properties.

At the end of the experiment, the glass powders are thoroughly rinsed in DI water to ensure that precipitates do not form after the end of the experiment.

SEM analysis

A field emission Scanning Electron Microscope (SEM) Zeiss Gemini Supra 55, JEOL JSM 6330 F was used to observe cross-sections of the altered glass grains to measure the thickness of their altered layers. The glass grains were set in an epoxy resin overnight and polished to a surface roughness of less than 1 µm before SEM observation. The polished resins were mounted on a metallic sample holder with an aluminum tape connecting the observable surface with the bottom of the sample holder and coated with carbon (a few nm) for image acquisition. The SEM images show the cross-sections of altered grains with an unaltered glass core surrounded by an altered gel layer of varying thicknesses. This method allows observing the cross-section of the altered grains.

NMR Characterization

A Bruker 500WB Avance II spectrometer, at 11.72 T magnetic field, was used for NMR data acquisition. A 4-mm Bruker CP-MAS probe at a spinning frequency of 12.5 kHz was used. Quantitative spectra of ^{27}Al, ^{23}Na, and ^{11}B were acquired using a short single pulse excitation of 1 µs in length with a tip angle of about 15°–20°. The recycle delay for ^{27}Al and ^{23}Na was 1 s, and for ^{11}B, it was 2 s. A rotor-synchronized spin echo-pulse sequence, consisting of a spin echo delay of one rotor period and soft selective pulses on the central transition, was used for ^{17}O MAS NMR spectra acquisition to minimize the baseline distortion due to the ringing signal. A Z-filter three-pulse sequence[43] was used for ^{17}O two-dimensional MQMAS spectra. Z-filter and RIACT two pulse sequences, detailed in literature[65,66], were used for optimal acquisition of the BO_4 and BO_3 peaks, respectively, in the ^{11}B MQMAS experiments. For $\{^{11}B/^{23}Na/^{27}Al, ^{1}H\}$ REDOR experiments, soft selective 90° and 180° pulses, of radio frequency 10–20 kHz and 180° pulse duration of 8–10 µs, were applied on the observed nuclei's (^{11}B, ^{23}Na and ^{27}Al) central transition ($1/2 \leftrightarrow 1/2$), and a rotor-synchronized train of 180° pulses of 9 µs in length were applied for ^{1}H[67–69]. A 90° pulse after a presaturation period, composed of a train of about twenty 90° pulses with a 2 ms delay between the pulses, and a recycle delay of 20 s was used for the ^{29}Si MAS NMR spectra. Chemical shifts of ^{11}B, ^{27}Al, ^{23}Na, and ^{29}Si were referenced to external samples of 1 M boric acid solution (19.6 ppm), 1 M $AlCl_3$ solution (0 ppm), 1 M NaCl solution (0 ppm) and powder of tetrakistrimethylsilane (−9.9 ppm) respectively. All data were processed and fitted using in-house software (T. Charpentier) with procedures described in literature[18,65,66].

Data availability

Data is provided within the manuscript or supplementary information files. Raw data can be provided upon reasonable request.

Received: 12 September 2024; Accepted: 20 December 2024;
Published online: 15 January 2025

References

1. *Status and Trends in Spent Fuel and Radioactive Waste Management*, no. NW-T-1.14 (Rev. 1). INTERNATIONAL ATOMIC ENERGY AGENCY, Vienna, 2022. [Online]. Available: https://www.iaea.org/publications/14739/status-and-trends-in-spent-fuel-and-radioactive-waste-management.
2. "Website published by "l'Agence Nationale pour la gestion des Déchets Radioactifs (Andra)"." https://www.andra.fr/.
3. Gin, S. et al. An international initiative on long-term behavior of high-level nuclear waste glass. *Mater. Today* **16**, 243–248 (2013).
4. Jantzen, C. M. in *Woodhead Publishing Series in Energy.* (eds Rashid Khan, M. & C. T. Ojovan) 230–292 (Woodhead Publishing, 2011).
5. Gin, S., Jollivet, P., Tribet, M., Peuget, S. & Schuller, S. Radionuclides containment in nuclear glasses: an overview. *Radiochimica Acta* **105**, https://doi.org/10.1515/ract-2016-2658 (2017).
6. ANDRA-Collectif, Dossier d'options de sûreté—Partie après fermeture (DOS-AF), published by "l'Agence Nationale pour la gestion des Déchets Radioactifs (Andra)", (2016)
7. Curti, E., Crovisier, J. L., Morvan, G. & Karpoff, A. M. Long-term corrosion of two nuclear waste reference glasses (MW and SON68): a kinetic and mineral alteration study. *Appl. Geochem.* **21**, 1152–1168 (2006).
8. Gin, S., Frugier, P., Jollivet, P., Bruguier, F. & Curti, E. New insight into the residual rate of borosilicate glasses: effect of S/V and glass composition. *Int. J. Appl. Glas. Sci.* **4**, 371–382 (2013).
9. Gin, S., Beaudoux, X., Angéli, F., Jégou, C. & Godon, N. Effect of composition on the short-term and long-term dissolution rates of ten borosilicate glasses of increasing complexity from 3 to 30 oxides. *J. Non Cryst. Solids* **358**, 2559–2570 (2012).
10. Neeway, J. J. The alteration of the SON68 reference waste glass in silica saturated conditions and in the presence of water vapor. PhD thesis of University of Nantes, (2011).
11. Utton, C. A. et al. Dissolution of vitrified wastes in a high-pH calcium-rich solution. *J. Nucl. Mater*. **435**, https://doi.org/10.1016/j.jnucmat.2012.12.032 (2013).
12. Neeway, J. J. et al. Effect of composition on the corrosion behavior of 24 statistically-designed alkali-borosilicate waste glasses. *J. Nucl. Mater.* **586**, 154674 (2023).
13. Gin, S., Delaye, J.-M., Angeli, F. & Schuller, S. Aqueous alteration of silicate glass: state of knowledge and perspectives. *npj Mater. Degrad.* **5**, 42 (2021).
14. Lenting, C. et al. Towards a unifying mechanistic model for silicate glass corrosion. *npj Mater. Degrad*. **2**, https://doi.org/10.1038/s41529-018-0048-z (2018).
15. Gin, S. et al. Dynamics of self-reorganization explains passivation of silicate glasses. *Nat. Commun*. **9**, https://doi.org/10.1038/s41467-018-04511-2 (2018).
16. Gin, S. et al. A general mechanism for gel layer formation on borosilicate glass under aqueous corrosion. *J. Phys. Chem. C.* **124**, 5132–5144 (2020).
17. Collin, M., Fournier, M., Charpentier, T., Moskura, M. & Gin, S. Impact of alkali on the passivation of silicate glass. *npj Mater. Degrad.* **2**, 16 (2018).
18. Collin, M. et al. Structure of International Simple Glass and properties of passivating layer formed in circumneutral pH conditions. *npj Mater. Degrad.* **2**, 4 (2018).
19. Damodaran, K., Gin, S., Naranayasamy, S. & Delaye, J.-M. On the effect of Al on alumino-borosilicate glass chemical durability. *npj Mater. Degrad.* **7**, 46 (2023).
20. Mir, A. H. & Peuget, S. Using external ion irradiations for simulating self-irradiation damage in nuclear waste glasses: state of the art, recommendations and, prospects. *J. Nucl. Mater.* **539**, 152246 (2020).
21. Mendoza, C. et al. Oxide glass structure evolution under swift heavy ion irradiation. *Nucl. Instrum. Method. Phys. Res. Sect. B Beam Interact. Mater. Atoms* **325**, 54–65 (2014).
22. Peuget, S., Tribet, M., Mougnaud, S., Miro, S. & Jégou, C. Radiations effects in ISG glass: from structural changes to long-term aqueous behavior. *npj Mater. Degrad.* **2**, 23 (2018).
23. Peuget, S. et al. Irradiation stability of R7T7-type borosilicate glass. *J. Nucl. Mater.* **354**, 1–13 (2006).
24. Peuget, S. et al. Effect of alpha radiation on the leaching behaviour of nuclear glass. *J. Nucl. Mater.* **362**, 474–479 (2007).
25. Mougnaud, S. et al. Effect of low dose electron beam irradiation on the alteration layer formed during nuclear glass leaching. *J. Nucl. Mater.* **482**, 53–62 (2016).
26. Mougnaud, S. et al. Heavy ion radiation ageing impact on long-term glass alteration behavior. *J. Nucl. Mater.* **510**, 168–177 (2018).
27. Gin, S. et al. Effects of irradiation on the mechanisms controlling the residual rate of an alumino-borosilicate glass. *npj Mater. Degrad.* **6**, 59 (2022).
28. Jan, A. et al. Radiation effects on the structure and alteration behavior of an SiO_2–Al_2O_3–B_2O_3–Na_2O glass. *Int. J. Appl. Glas. Sci.* **14**, 113–132 (2023).
29. Lönartz, M. I. et al. The effect of heavy ion irradiation on the forward dissolution rate of borosilicate glasses studied in situ and real time by fluid-cell Raman spectroscopy. *Materials* **12**, https://doi.org/10.3390/ma12091480 (2019).
30. Gillet, C., Szenknect, S., Tribet, M., Arena, H. & Peuget, S. Impact of gold ion irradiation on the initial alteration rate of the International Simple Glass. *J. Nucl. Mater.* **588**, 154817 (2024).
31. Gin, S., Taron, M., Arena, H. & Delaye, J.-M. Effect of structural disorder induced by external irradiation with heavy ions on the alteration of a four oxide borosilicate glass. *npj Mater. Degrad.* **8**, 64 (2024).
32. Filippov, A., Antzutkin, O. N. & Shah, F. U. Understanding the interaction of boric acid and CO2 with ionic liquids in aqueous medium by multinuclear NMR spectroscopy. *ACS Sustain. Chem. Eng.* **8**, 552–560 (2020).

33. Schott, J. et al. Formation of a Eu(iii) borate solid species from a weak Eu(iii) borate complex in aqueous solution. *Dalt. Trans.* **43**, 11516–11528 (2014).
34. Narayanasamy, S. et al. Borosilicate glass alteration in vapor phase and aqueous medium. *npj Mater. Degrad.* **6**, 86 (2022).
35. Alloteau, F. et al. New insight into atmospheric alteration of alkali-lime silicate glasses. *Corros. Sci.* **122**, 12–25 (2017).
36. Barrow, N. et al. MAS-NMR studies of carbonate retention in a very wide range of Na2O-SiO2 glasses. *J. Non Cryst. Solids* **534**, 119958 (2020).
37. Reeve, Z. E. M. et al. Detection of electrochemical reaction products from the sodium–oxygen cell with solid-state 23Na NMR spectroscopy. *J. Am. Chem. Soc.* **139**, 595–598 (2017).
38. Angeli, F., Gaillard, M., Jollivet, P. & Charpentier, T. Influence of glass composition and alteration solution on leached silicate glass structure: a solid-state NMR investigation. *Geochim. Cosmochim. Acta* **70**, 2577–2590 (2006).
39. Yesinowski, J. P., Eckert, H. & Rossman, G. R. Characterization of hydrous species in minerals by high-speed proton MAS-NMR. *J. Am. Chem. Soc.* **110**, 1367–1375 (1988).
40. Jin, X. et al. Selective mass transport mediated by two-dimensional confined water: a comprehensive review. *FlatChem* **47**, 100708 (2024).
41. Angeli, F., Charpentier, T., Gin, S. & Petit, J. C. 17O 3Q-MAS NMR characterization of a sodium aluminoborosilicate glass and its alteration gel. *Chem. Phys. Lett.* **341**, 23–28 (2001).
42. Angeli, F., Charpentier, T., Gaillard, M. & Jollivet, P. Influence of zirconium on the structure of pristine and leached soda-lime borosilicate glasses: towards a quantitative approach by 17O MQMAS NMR. *J. Non Cryst. Solids* **354**, 3713–3722 (2008).
43. Massiot, D. et al. Two-dimensional magic-angle spinning isotropic reconstruction sequences for quadrupolar nuclei. *Solid State Nucl. Magn. Reson.* **6**, 73–83, https://doi.org/10.1016/0926-2040(95)01210-9 (1996).
44. Fernandez, C. & Amoureux, J. P. Triple-quantum MAS-NMR of quadrupolar nuclei. *Solid State Nucl. Magn. Reson.* **5**, 315–321, https://doi.org/10.1016/0926-2040(95)01197-8 (1996).
45. Tribet, M. et al. Irradiation impact on the leaching behavior of HLW glasses. *Procedia Mater. Sci.* **7**, 209–215 (2014).
46. Tribet, M. et al. New Insights about the importance of the alteration layer/glass interface. *J. Phys. Chem. C.* **124**, 10032–10044 (2020).
47. Maugeri, E. A. et al. Calorimetric study of glass structure modification induced by α decay. *J. Am. Ceram. Soc.* **95**, 2869–2875 (2012).
48. Peuget, S., Delaye, J.-M. & Jégou, C. Specific outcomes of the research on the radiation stability of the French nuclear glass towards alpha decay accumulation. *J. Nucl. Mater.* **444**, 76–91 (2014).
49. Mir, A. H., Monnet, I., Boizot, B., Jégou, C. & Peuget, S. Electron and electron-ion sequential irradiation of borosilicate glasses: Impact of the pre-existing defects. *J. Nucl. Mater.* **489**, 91–98 (2017).
50. Tribet, M. et al. Alpha dose rate and decay dose impacts on the long-term alteration of HLW nuclear glasses. *npj Mater. Degrad.* **5**, 36 (2021).
51. Gin, S. et al. Atom-probe tomography, TEM and ToF-SIMS study of borosilicate glass alteration rim: a multiscale approach to investigating rate-limiting mechanisms. *Geochim. Cosmochim. Acta* **202**, https://doi.org/10.1016/j.gca.2016.12.029 (2017).
52. Kaya, H., Gin, S., Vogt, B. D. & Kim, S. H. Impact of aqueous solution pH on network structure of corrosion-induced surface layers of boroaluminosilicate glass. *J. Am. Ceram. Soc.* **105**, 6581–6592 (2022).
53. Taron, M. Simulation à l'échelle Nanoscopique du Transport Réactif: Application à la Dissolution des Verres Nucléaires (2022). [Online]. Available at: http://www.theses.fr/2022UMONS017/document.
54. Collin, M. Géochimie en Milieu Nanoporeux: Application aux verres Nucléaires (Université de Montpellier, 2018). [Online]. Available at: https://theses.hal.science/tel-02195581.
55. Rebiscoul, D. et al. Morphological evolution of alteration layers formed during nuclear glass alteration: new evidence of a gel as a diffusive barrier. *J. Nucl. Mater.* **326**, 9–18 (2004).
56. Ngo, D. et al. Hydrogen bonding interactions of H2O and SiOH on a boroaluminosilicate glass corroded in aqueous solution. *npj Mater. Degrad.* **4**, 1 (2020).
57. Risplendi, F., Raffone, F., Lin, L.-C., Grossman, J. C. & Cicero, G. Fundamental insights on hydration environment of boric acid and its role in separation from saline water. *J. Phys. Chem. C.* **124**, 1438–1445 (2020).
58. Gillet, C. Etude des Effets de Synergie Entre Irradiation et Altération Par l'eau des Verres Nucléaires. (Université de Montpellier, 2022). [Online]. Available: https://theses.hal.science/tel-04116088.
59. Madani, S. H. et al. Pore size distributions derived from adsorption isotherms, immersion calorimetry, and isosteric heats: a comparative study. *Carbon N. Y.* **96**, 1106–1113 (2016).
60. Assoualaye, G. & Djongyang, N. Influence of pore size and isosteric heat of adsorption of some metal–organic frameworks on the volumetric and gravimetric adsorption capacities of hydrogen at room temperature. *Polym. Bull.* **78**, 4987–5001 (2021).
61. Fournier, M., Gin, S. & Frugier, P. Resumption of nuclear glass alteration: state of the art. *J. Nucl. Mater.* **448**, 348–363 (2014).
62. Fournier, M., Gin, S., Frugier, P. & Mercado-Depierre, S. Contribution of zeolite-seeded experiments to the understanding of resumption of glass alteration. *npj Mater. Degrad.* **1**, https://doi.org/10.1038/s41529-017-0018-x (2017).
63. Fournier, M. et al. Glass dissolution rate measurement and calculation revisited. *J. Nucl. Mater.* **476**, 140–154 (2016).
64. Fournier, M. et al. Reactive surface of glass particles under aqueous corrosion. *Procedia Earth Planet. Sci.* **17**, 257–260 (2017).
65. Hopf, J. et al. Glass–water interaction: effect of high-valence cations on glass structure and chemical durability. *Geochim. Cosmochim. Acta* **181**, 54–71 (2016).
66. Angeli, F., Charpentier, T., De Ligny, D. & Cailleteau, C. Boron speciation in soda-lime borosilicate glasses containing zirconium. *J. Am. Ceram. Soc.* **93**, 2693–2704 (2010).
67. Angeli, F. et al. Effect of thermally induced structural disorder on the chemical durability of International Simple Glass. *npj Mater. Degrad.* **2**, 31 (2018).
68. Bertmer, M., Züchner, L., Chan, J. C. C. & Eckert, H. Short and medium range order in sodium aluminoborate glasses. 2. Site connectivities and cation distributions studied by rotational echo double resonance NMR spectroscopy. *J. Phys. Chem. B* **104**, 6541–6553 (2000).
69. Janssen, M. & Eckert, H. 11B{23Na} Rotational echo double resonance NMR: a new approach for studying the spatial cation distribution in sodium borate glasses. *Solid State Ion.* **136–137**, 1007–1014 (2000).

Acknowledgements

Sincere thanks to Marie Fenart (DES/ISEC/DPME/SEME/LEMC, CEA Marcoule) for the SEM images and help with the sample preparation. This work was supported as part of the Center for Performance and Design of Nuclear Waste Forms and Containers, an Energy Frontier Research Center funded by the U.S. Department of Energy, Office of Science, Basic Energy Sciences under Award Number: DE-SC0016584.

Author contributions

S.G., T.C., J.M.D., and A.J. conceptualized the study. A.J. performed the glass alteration experiments. T.C., M.M., and M.B. conducted the NMR experiments. S.N. prepared the samples for SEM analysis. T.C., S.N., and S.G. performed data analysis and interpretation. S.G. and J.M.D. supervised the study. S.N. wrote the main manuscript text. S.G., T.C., J.M.D., A.J., and S.N. reviewed the manuscript.

Competing interests

Authors S.N., T.C., J.M.D., A.J., M.M., and M.B. declare no financial or non-financial competing interests. Author S.G. serves as Editor-in-Chief

of this journal and had no role in the peer-review or decision to publish this manuscript. Author S.G. declares no financial competing interests.

Additional information

Supplementary information The online version contains supplementary material available at https://doi.org/10.1038/s41529-024-00550-x.

Correspondence and requests for materials should be addressed to Sathya Narayanasamy.